The Unsteady Temperature Field in a Turbine Blade Cooling Channel

T. Arts
Von Karman Institute for Fluid Dynamics
72, chausse de Waterloo
13 1640 Rhode Saint Genese
Belgium

Y. Kinoue
Dept. of Mechanical Engineering
Saga University
Honjo 1
Saga 840 8502
Japan

M.T. Abad-Lozano
Volkswagen Research
Engine Thermodynamics
Letterbox 1778/1
38436 Wolfsburg
Germany

S. Pierret
Numeco International
Optimization Group
Avenue Franklin Roosevelt 5
B-1050 Brussels
Belgium

Abstract

The unsteady velocity and temperature fields are measured in a straight smooth and rib roughened square duct, representative of a stator cooling channel. The mainstream Reynolds number is 3 10^4. Single cold and hot wire probes as well as a dual hot/cold wire probe are used for this purpose. The experimental results are compared to the predictions from FINE, a commercial software package developed by Numeca International. This research work was performed while the second and third author were in residence at the von Karman Institute

Introduction

The improvement of gas turbine performance is intimately linked to the optimization of each individual component, especially in the high-pressure turbine, which is submitted to high thermal loads. The development and validation of numerical methods allowing to predict the metal temperature distribution, as well as the associated convective heat transfer, are absolutely needed in order to determine the life time of blades, endwalls, disks, etc… Considering the complexity of this numerical simulation, an experimental approach still provides a lot of useful results in this area. It delivers information directly applicable in the design process of the components, allows to verify their performance and finally contributes to the development of a database for CFD validation.

The classical way to improve the thermal efficiency of a gas turbine cycle is to increase the turbine entry temperature. The latter is usually much higher than the allowable metal temperature. Efficient cooling techniques are therefore absolutely required. One of the commonly used approaches is internal convection cooling. The cooling air, usually drawn from the compressor, is flown through narrow straight or serpentine passages inside the stator and rotor airfoils and blown out at several locations. Turbulence promoters such as ribs or pin fins are provided on one or more surfaces of these passages in order to enhance significantly the heat transfer distribution. As the minimum rib dimensions are usually limited by manufacturing constraints, and considering the ever-increasing freestream temperatures, the coolant flow is more and more often subjected to high blockage, i.e. larger ribs in smaller channels.

Paper presented at the RTO AVT Symposium on "Advanced Flow Management: Part B – Heat Transfer and Cooling in Propulsion and Power Systems", held in Loen, Norway, 7-11 May 2001, and published in RTO-MP-069(I).

Report Documentation Page

Form Approved
OMB No. 0704-0188

1. REPORT DATE	2. REPORT TYPE	3. DATES COVERED
00 MAR 2003	**N/A**	**-**

4. TITLE AND SUBTITLE	5a. CONTRACT NUMBER
The Unsteady Temperature Field in a Turbine Blade Cooling Channel	5b. GRANT NUMBER
	5c. PROGRAM ELEMENT NUMBER
6. AUTHOR(S)	5d. PROJECT NUMBER
	5e. TASK NUMBER
	5f. WORK UNIT NUMBER
7. PERFORMING ORGANIZATION NAME(S) AND ADDRESS(ES) **NATO Research and Technology Organisation BP 25, 7 Rue Ancelle, F-92201 Neuilly-Sue-Seine Cedex, France**	8. PERFORMING ORGANIZATION REPORT NUMBER
9. SPONSORING/MONITORING AGENCY NAME(S) AND ADDRESS(ES)	10. SPONSOR/MONITOR'S ACRONYM(S)
	11. SPONSOR/MONITOR'S REPORT NUMBER(S)

12. DISTRIBUTION/AVAILABILITY STATEMENT
Approved for public release, distribution unlimited

13. SUPPLEMENTARY NOTES
Also see ADM001490, presented at RTO Applied Vehicle Technology Panel (AVT)Symposium held in Leon, Norway on 7-11 May 2001, The original document contains color images.

14. ABSTRACT

15. SUBJECT TERMS

16. SECURITY CLASSIFICATION OF:			17. LIMITATION OF ABSTRACT	18. NUMBER OF PAGES	19a. NAME OF RESPONSIBLE PERSON
a. REPORT **unclassified**	b. ABSTRACT **unclassified**	c. THIS PAGE **unclassified**	**UU**	**14**	

The flow regime in these cooling channels is definitely turbulent. In order to understand the convection phenomena, the characteristics of the turbulent temperature field, such as temperature fluctuation intensities and turbulent heat fluxes should definitely be examined in details. Hirota et al. (1997) provided a detailed analysis of these quantities in a smooth straight duct with a square cross-section. Similar information within rib roughened channels, especially for high blockage ratios, seems however to be quite scarce in the open literature. Han (1984) proposed a simple correlation, based one a one-dimensional analysis, to predict the surface heat transfer for low blockage ratios ($e/D_h < 0.0625$). The measurements conducted by Rau et al (1998) proved however that this correlation could not be applied anymore for larger rib heights. Similar data were provided by Taslim et al (1994) for $e/D_h = 0.167$, by Taslim and Wadworth (1997) and Korotky (1996) for $e/D_h = 0.133 \ldots 0.25$ and by recently by Çakan (2000) for $e/D_h = 0.3$. In this environment, the importance of the three-dimensional nature of the flow strongly increases. These measurements put in evidence not only the recirculation bubbles existing in front, on top and behind the ribs but also structures such as pairs of contra-rotating longitudinal vortices covering the entire channel cross-section. However, flow temperature data (steady and unsteady) in these high blockage configurations are not available in the open literature.

The objective of the paper is therefore to provide additional aero-thermal data in these high blockage ratio cooling channels and to compare them with the predictions from a commercial software package, FINE, developed by Numeca International. In a first part, the analysis is conducted in a smooth unribbed straight channel, in order to validate the approach against the data of Hirota et al (1997). The second part of the paper deals with a roughened straight channel, with ribs presenting a high blockage ratio (30 %). In the present paper, the measurements are conducted in the symmetry plane of the channel.

Experimental apparatus

A schematic of the test setup is shown in Fig. 1. Air at ambient temperature and atmospheric pressure is aspirated by means of a blower through a straight channel (length = 3 m) with a square cross-section (0.1×0.1 m^2). The bulk velocity is set at 6 m/s, corresponding to a Reynolds number value, based on the hydraulic diameter of the channel, of $3\ 10^4$. The setup is characterized by an unheated starting length of 1 m and a heated part of 2 m. The heating is provided by a thin (25 μm) Inconel sheet glued on one wall. This approach allows to enforce a uniform heat flux thermal boundary conduction. Conduction and radiation losses are taken into account to obtain the correct value of the convective heat flux. A detailed description of the test section is provided by Rau et al (1998) and Çakan (2000). The ribs are made out of Plexiglas, and covered with the same heating element. They have a square section (0.03×0.03 m^2), i.e. $e/D_h = 0.3$, and are placed perpendicularly to the freestream direction. Six ribs are used; the rib pitch to height ratio is equal to 10. As indicated in Fig. 1, all measurements are taken between the 4th and the 5th rib, where the flow conditions are expected to be periodical.

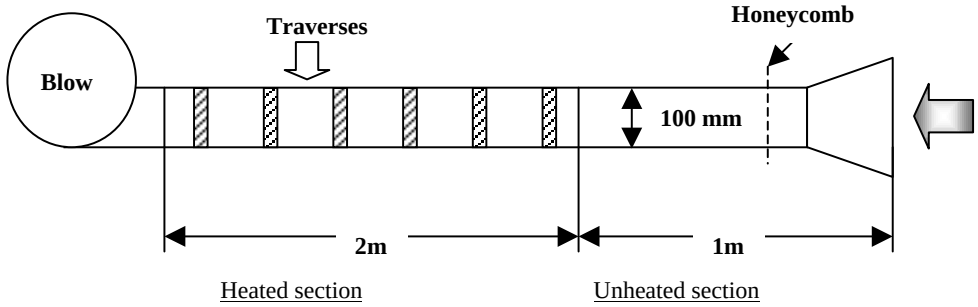

Fig. 1 – Schematic view of the test section

The time-resolved freestream flow temperature is obtained by means of cold wire thermometry. Frequency compensation must be applied in order to correct the unsteady conduction phenomena between wire and prongs, as suggested by Dénos and Sieverding (1997). The signal is sampled at a frequency of 20 kHz. The velocity measurements are performed by means of hot wire anemometry. Simultaneous measurements are taken in addition with a dual hot/cold wire probe. The two wires are parallel, with the cold wire placed upstream (from a flow direction point of view) of the hot one. The comparison of the single and dual probe measurements demonstrates that no spurious interaction between the wires could be put in evidence. The characteristics of the 3 probes are presented in Table 1.

CHARACTERISTICS	Single Cold Wire	Single Hot Wire	Dual Probe	
			Cold Wire	Hot Wire
Wire Diameter [μm]	2.5	9	2.5	9
Distance prongs [mm]	0.73	1.9	0.85	1.5
Active Length [mm]	0.73	1.9	0.85	1.5
Dynamic response [kHz]	1	15	1	15
Resistance [Ω]	~7.0	~2.4	~6.8	~2.3

Table 1 – Probe characteristics

Velocity and temperature traverses are made perpendicularly to the heated smooth or ribbed wall in the longitudinal symmetry plane of the channel. The different measurement planes of the ribbed channel are defined in Fig. 2; they are located at respectively 1, 3, 4, 5, 7 rib heights downstream of the rear face of the 4th rib. An additional measurement plane is defined on top of the 5th rib. Control thermocouples are used to determine the local mean temperature at the wall and along the axis of the channel in order to normalize the data obtained from the cold wire.

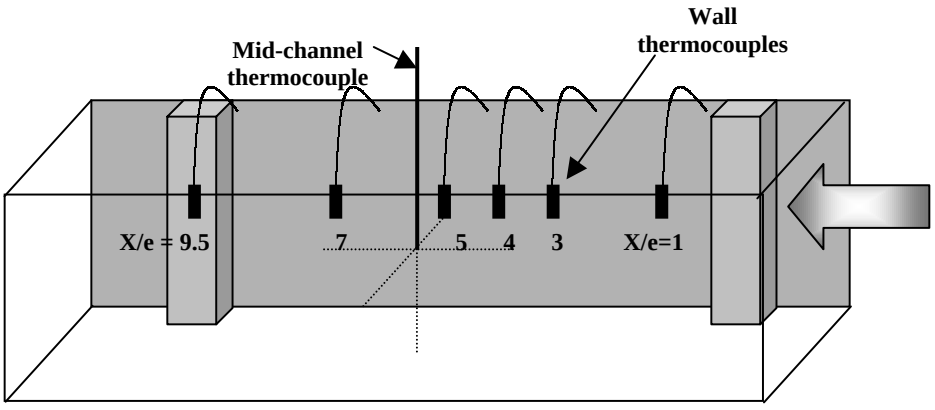

Fig. 2 – Definition of measurement planes

The uncertainties associated to the measurements are evaluated to be 0.5 deg and 0.35 deg, respectively for the mean and fluctuating values of the temperature and 0.09 m/s for the fluctuating component of the velocity.

Numerical predictions

The FINE code, developed by Numeca International, is used to provide numerical predictions. It is a multi-purpose solver for 2D and 3D flows. Structured meshes are used and complex geometries can be handled through a multi-block meshing procedure. In the present low speed application, the Reynolds-averaged Navier-Stokes equations are solved with the help of a preconditioning method based on a pseudo compressibility approach. The space discretization is based on a finite volume approach whereas the time discretization uses a multi-stage Runge-Kutta procedure. The combination of multigrid and implicit residual averaging procedures is used for convergence acceleration. More detailed information about the solver is provided by Hirsch et al (1991, 1995).

Different turbulence models were considered, namely the well known algebraic Baldwin-Lomax (1978) model, a standard k-ε model (Launder and Spalding, 1974), a low Reynolds number k-ε model (Yang and Shih, 1993) and a non linear k-ε model, based on the Yang-Shih model (Hirsch and Khodak, 1995). Wall functions were used in the case of the standard k-ε model.

The comparisons between measurements and calculations presented in this paper exclusively concern the flow temperature field, which is undoubtly the most difficult quantity to predict. Comparisons between the kinematic fields, expressed in terms of velocity distributions, separation or reattachment lengths … are generally good, demonstrating the ability of FINE to handle this part of the flowfield. However, due to space limitations and because additional PIV measurements are presently underway at the VKI, a detailed discussion of the velocity field will be presented in the near future.

Results in the smooth channel

Mean profiles

Fig. 3 shows part of the 2D and 3D meshes used for the calculations with FINE. The number of grid points are respectively equal to 81×49 (2D) and 81×49×49 (3D); this corresponds to y^+ values of the first cell respectively equal to 3.0 (2D) and 5.0 (3D). A $1/7^{th}$ power law is used to define the inlet velocity profile. The other quantities (inlet temperature, wall heat flux and Reynolds number) are derived from the measured values.

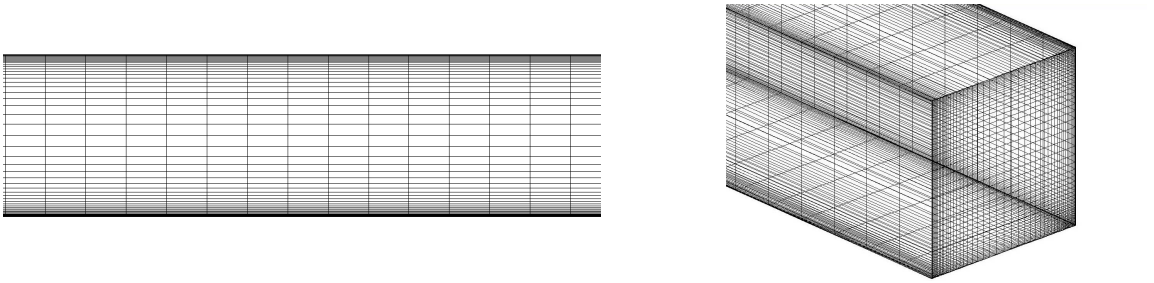

Fig. 3 – 2D and 3D grids used for the FINE calculations in the smooth channel

The measured and calculated mean temperature profiles are compared to values extracted from literature (Hirota et al, 1997 and Kays and Crawford, 1980) in Figs. 4 (2D computations) and 5 (3D computations); wall coordinates (y^+ and T^+) are used for this purpose:

$$T^+ = -\rho C_p u_\tau \frac{T - T_{wall}}{q_{wall}} \qquad y^+ = \frac{y u_\tau}{\nu} \tag{1}$$

The measured values agree quite well with the values from literature, giving confidence in the experimental approach. The 2D predictions with FINE (in the present case with the non-linear k-ε model) also agree with the measurements but only for values of y^+ larger than 30 (Fig. 4). Closer to the wall the predictions are worse. Similar conclusions are drawn when the other turbulence models are used. This could be due either to an insufficient grid resolution or to an incorrect thermal turbulence modeling near the wall. Measurements from Hishida (1986), confirmed by some LDV measurements in the present setup at VKI, indeed show that the turbulent Prandtl number is not constant close to the wall. The 3D computations reveal a relatively poor performance of the Baldwin-Lomax model and, up to some extent, of the standard k-ε model (Fig. 5).

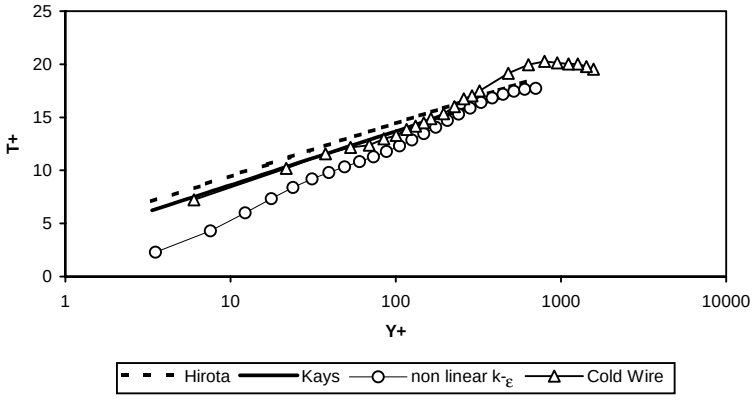

Fig. 4 – Mean temperature profiles – Measurements and 2D computations

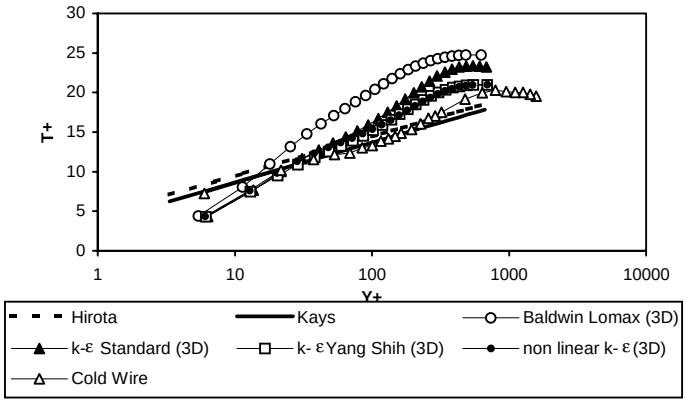

Fig. 5 – Mean temperature profiles – Measurements and 3D computations

RMS profiles

The measured RMS profiles of temperature and streamwise velocity (single and dual probes) are plotted in Figs. 6 and 7 whereas the velocity-temperature correlation (dual probe) is presented in Fig. 8. The RMS values are defined as follows:

$$T^*_{RMS} = \frac{T_{RMS}}{T_{wall} - T_{mid}} \qquad U^*_{RMS} = \frac{U_{RMS}}{U_{mid}} \qquad \left(\overline{u'T'}\right)^* = -100\frac{\left(\overline{u'T'}\right)}{U_{mid}\left(T_{wall} - T_{mid}\right)} \quad (2)$$

The subscripts (mid) and (wall) refer to the values measured respectively on the wall and along the axis of the channel. Good agreement is again observed with the data of Hirota et al. The present measurements provide however better resolution near the wall.

The hot wire probe used in the present test campaign does not allow the determination of the velocity component normal to the wall. The turbulent heat flux can therefore not be measured. Only the comparison between the results from FINE and the data from Hirota et al is therefore presented in Fig. 9, according to the following expression:

$$\left(\overline{v'T'}\right) = -\varepsilon_H \frac{\partial T}{\partial y} = -\frac{\varepsilon_M}{Pr_t}\frac{\partial T}{\partial y} \tag{3}$$

where ε_M and ε_H are the eddy diffusivities for momentum and heat and Pr_t is the turbulent Prandtl number. The results from FINE agree quite well with the data from Hirota for y/D_h values larger than 0.2. Closer to the wall, large discrepancies are however observed. As mentioned earlier, this could be due to insufficient grid resolution or, much more probably, to the effect of Pr_t variations near the wall. Additional LDV measurements, not reported in the present contribution, show indeed large values of Pr_t in this region; the calculations therefore largely overestimate the turbulent heat flux.

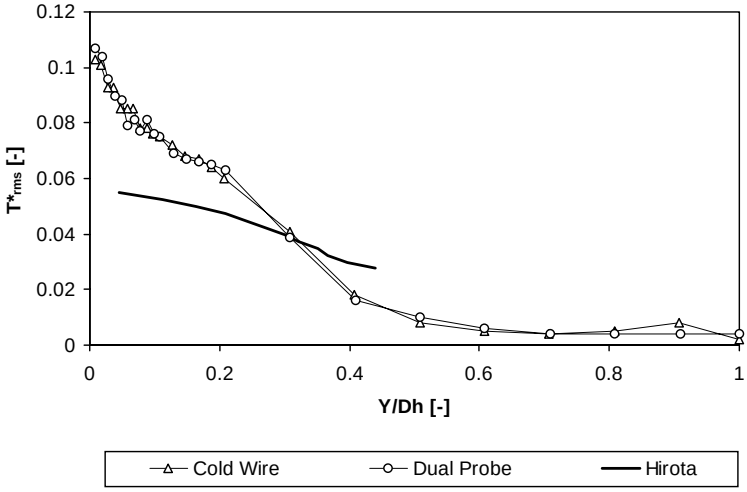

Fig. 6 – RMS temperature profiles (Measurements)

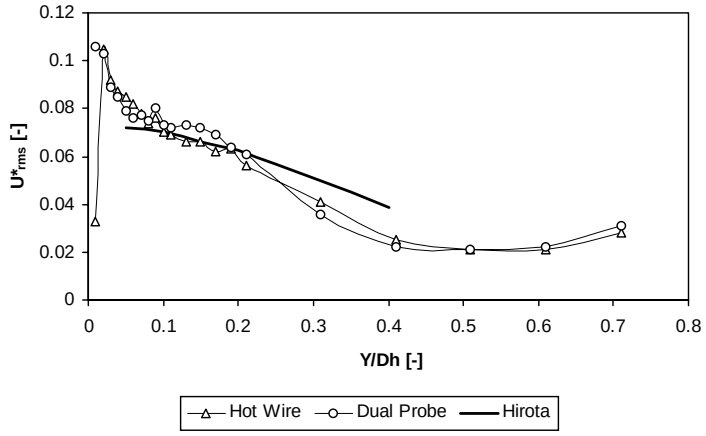

Fig. 7 – RMS streamwise velocity profiles (Measurements)

From the author's experience, this overestimation is also observed with other software packages. It therefore definitely calls for more accurate thermal turbulence models in the existing solvers.

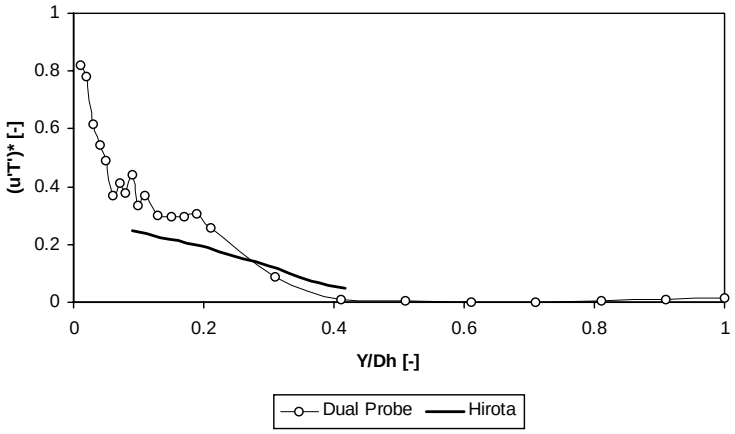

Fig. 8 – Velocity/Temperature correlation profiles (Measurements)

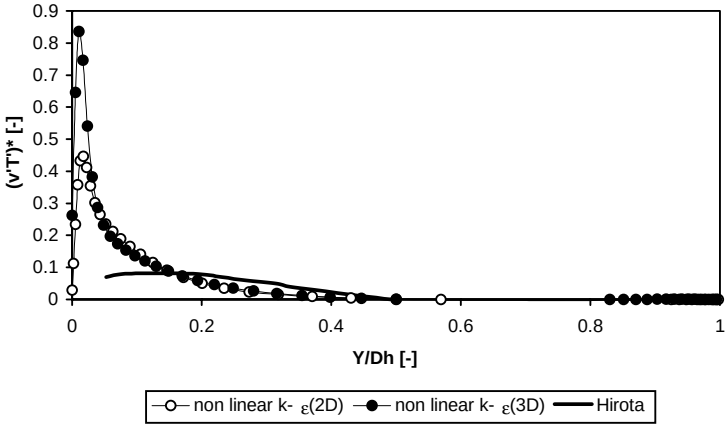

Fig. 9 – Turbulent heat flux profiles (Computations)

Results in the ribbed channel

Mean and RMS temperature profiles

The mean temperature profiles in the 6 measurement planes are presented in Fig. 10; the dotted line shows the upper surface position of the rib. These measurements are obtained from the single cold wire probe. The values of temperature are normalized as follows:

$$T^* = \frac{T - T_{mid}}{T_{wall} - T_{mid}} \tag{4}$$

The mean flowfield is expected to be characterized by a large recirculation zone downstream of the rib, a reattachment (X/e ~ 3.5 … 4.0), the development of a new boundary layer, a separation upstream of the next rib and a separation on top of the rib (Rau et al, 1998). In the plane X/e = 1, including the first recirculation zone, the mean temperature profile is relatively characteristic. The highest temperatures are measured close to the wall and a large temperature gradient is observed around $y/D_h = 0.3$ (the upper surface of the rib). Similar characteristics are

observed in the planes X/e = 3 and 4. In planes X/e = 5 and 7 the larger temperature gradients around the rib height have disappeared. At X/e = 9.5, i.e. on top of the rib, high temperature gradients close to the surface are again identified.

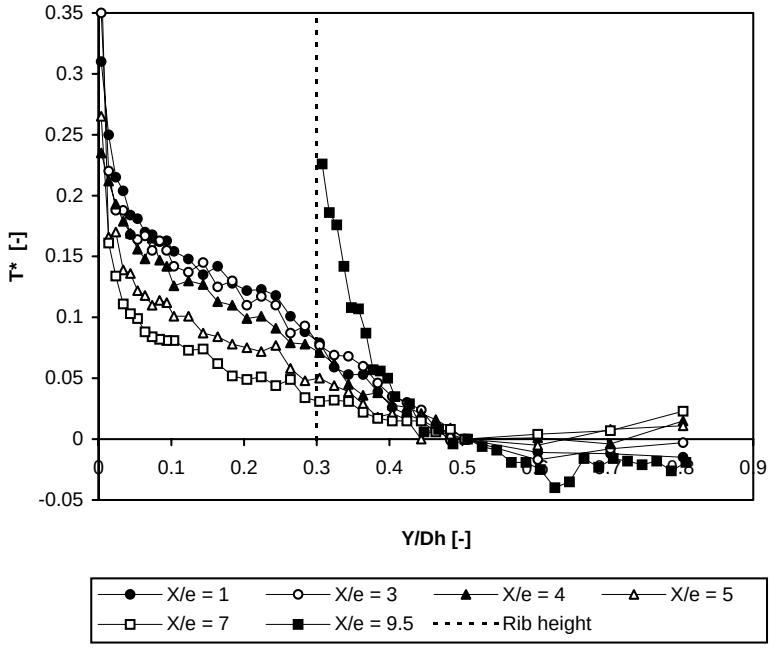

Fig. 10 – Mean temperature profiles in the ribbed channel (measurements)

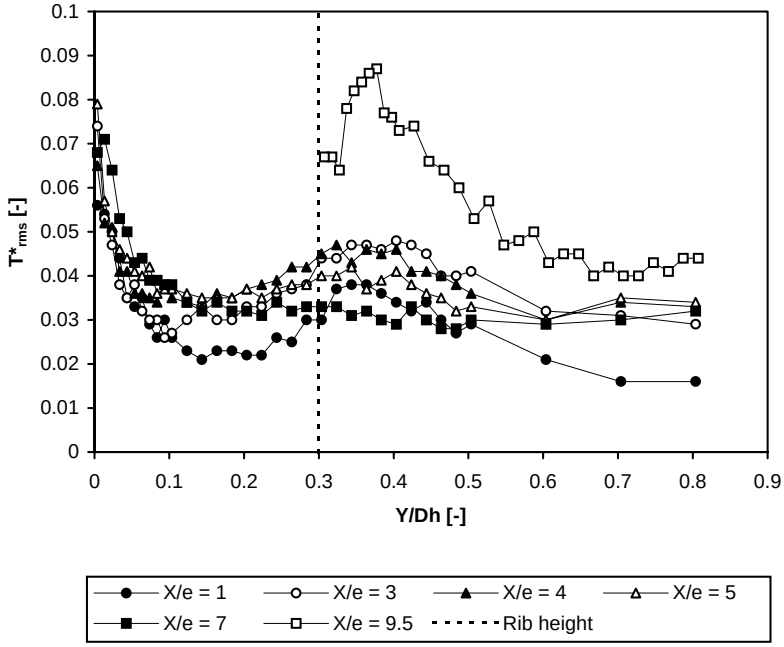

Fig. 11 - RMS temperature profiles in the ribbed channel (measurements)

The RMS temperature profiles are presented in Fig. 11. The values are normalized as in the preceding section (equ. 2). Besides the high RMS value near the wall, a second maximum is identified around $y/D_h = 0.35$, i.e. slightly above the rib, for the planes X/e = 1, 3 and 4. This seems to be correlated to the higher mean temperature gradients observed in the same area, and therefore to the recirculating region. In addition, the height of this peak does not vary a lot in the streamwise direction. In the planes X/e = 5 and 7, located downstream of the reattachment point, this second maximum is not observed anymore.

RMS velocity and temperature profiles

The comparison between the RMS velocity and temperature profiles in the planes X/e=1, 3 and 4 is presented in Figs 12 to 14. The values are normalized as in the preceding section (equ. 2). The location of the maximum in U_{RMS} appears to vary from $y/D_h = 0.3$, i.e. the rib height, at X/e =1 towards the wall when moving more downstream (X/e = 3 and 4), as expected from the mean shear layer behaviour downstream of the rib. The temperature, if considered as a passive scalar, should follow the same tendencies. This is not observed. Hishida et al (1986) performed similar measurements and observed similar tendencies. The reason for these different behaviours in fluctuating RMS temperature and velocity distributions is yet not fully understood. Let us finally remark that these measurements were made both with the single and the dual probe, optimizing the relative position of the two sensors in forward or return flow and leading to similar conclusions.

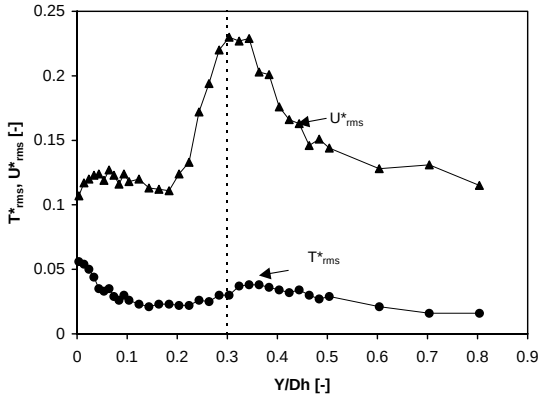

Fig.12 – RMS Velocity and Temperature distributions (X/e=1)

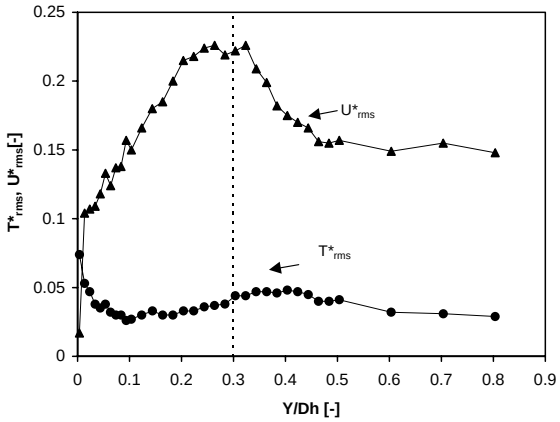

Fig.13 – RMS Velocity and Temperature distributions (X/e=3)

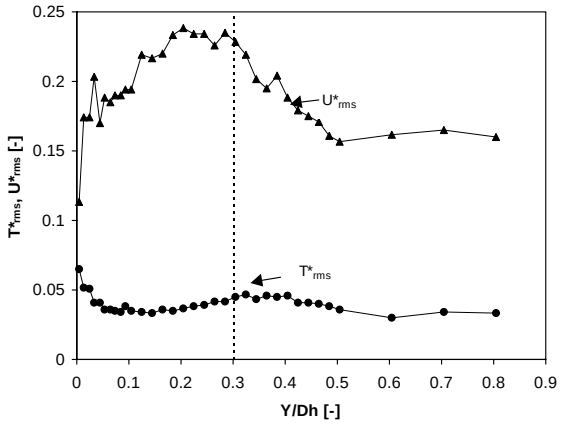

Fig.14 – RMS Velocity and Temperature distributions (X/e=4)

Numerical predictions

A portion of the 3D mesh used for the numerical predictions is presented in Fig. 15. The full channel is meshed; a multi-block strategy is applied. A total number of 642.209 grid points are used; the y^+ value of the first cell is about 2.5.

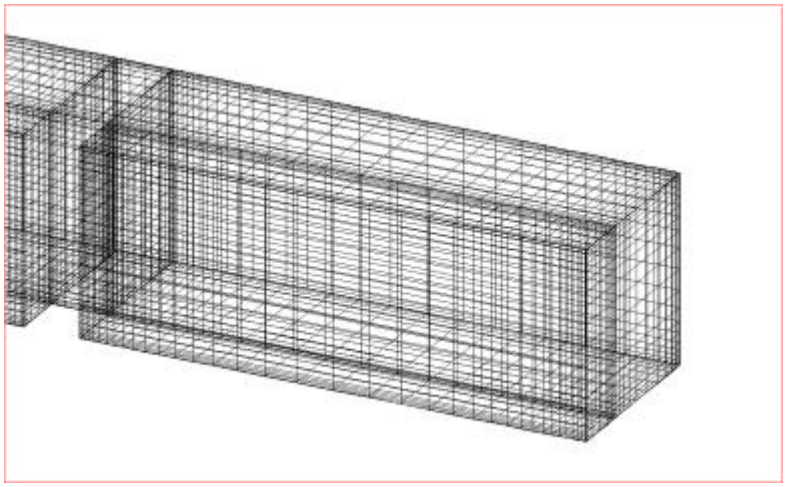

Fig. 15 – Portion of the 3D grid used for the FINE calculations in the ribbed channel

The standard k-ε turbulence model is used. The boundary conditions are extracted from the measurements. The reattachment point of the flow downstream of the rib is calculated at X/e= 3.66 (in the symmetry plane). This agrees quite well with the measurements from the dual probe. Typical mean temperature profiles are presented in Figs 16 and 17 respectively at X/e=1 and 5. The common characteristic between those results is that the gradients very close to the wall are not so well captured. Further away, the measurements agree quite well with the predictions. A comparison was also made with mean heat transfer coefficient distributions measured by Çakan (2000). The measured and calculated data agree quite well qualitatively along the ribbed wall; the quantitative comparison is however poorer.

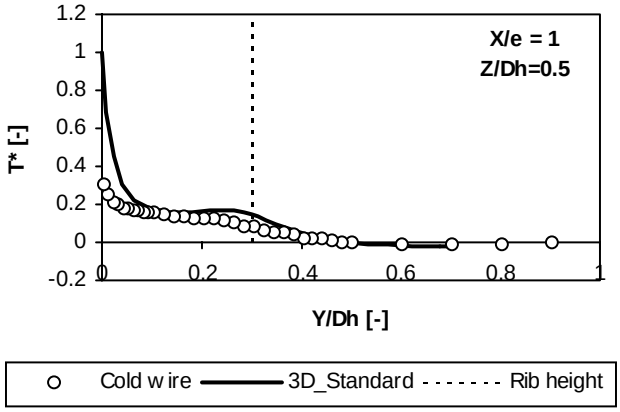

Fig. 16 – Measured and computed mean temperature profile (X/e=1)

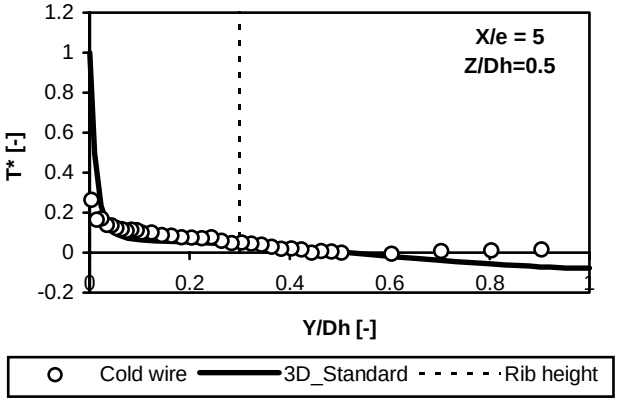

Fig. 17 – Measured and computed mean temperature profile (X/e=5)

Conclusions

The time-resolved velocity and temperature fields were measured in a smooth and rib roughened straight channel with a square cross-section. Single cold and hot wire probes as well as a dual cold/hot wire probe were used for this purpose. The measured results were compared with the predictions obtained from FINE, a commercial software package developed by Numeca International.

The measurements in the smooth channel agree quite well with data from the open literature. The velocity field is quite well predicted and reasonable agreement is also observed with the calculations of the mean temperature profiles. Turbulent heat flux predictions remain difficult to perform. More attention must definitely be devoted to the thermal turbulence modeling aspects, including anisotropy and variable turbulent Prandtl number effects.

The RMS velocity and temperature data seem to present different characteristics in the ribbed channel. The flow features identified in the present study are in good agreement with earlier data on similar configurations. The mean temperature profile predictions compare relatively well with the measurements, except in the close wall vicinity. The reattachment point downstream of the rib is also well predicted.

List of Symbols

C_p	specific heat at constant pressure
D_h	hydraulic diameter
E	rib height
Pr_t	turbulent Prandtl number
Q	heat flux
T	temperature
T’	fluctuating component of temperature
U	streamwise velocity
u’, v’	fluctuating component of streamwise and normal velocity
u_τ	friction velocity
x, y, z	coordinates
ε_H	eddy diffusivity for heat
ε_M	eddy diffusivity for momentum
ρ	density
υ	kinematic viscosity

Subscripts

mid	along the axis of the channel
RMS	root mean square
wall	at the wall

References

Baldwin, B.S. & Lomax, H. (1978): Thin Layer Approximation and Algebraic Model for Separated Turbulent Flows. AIAA Paper 78-0257

Çakan, M. (2000): Aero-Thermal Investigation of Fixed Rib-Roughened Internal Cooling Passages, Ph.D. Thesis, Université Catholique de Louvain, Belgium

Dénos, R. & Sieverding, C.H. (1997): Assessment of the Cold Wire Resistance Thermometer for High Speed Turbomachinery Applications. J. of Turbomachinery, ASME, Vol. 119, pp 140-148

Han, J.C. (1984): Heat Transfer and Friction on Channels with Two Opposite Rib-Roughened Walls. J. of Heat Transfer, ASME, Vol. 106, pp 774-781

Hirota, M.; Fujita, H.; Yokosawa, H.; Nakai, H.; Itoh, H. (1997): Turbulent Heat Transfer in a Square Duct. Int. J. of Heat and Fluid Flow, Vol. 18, pp 170-180

Hirsch, C.; Lacor, C.; Rizzi, A.; Eliasson, P.; Lindblad, I.; Hauser, J. (1991): A Multiblock/-Multigrid Code for the Efficient Solution of Complex 3D Navier-Stokes Flows. Proc. of the First European Symposium on Aerodynamics for Space Vehicles, pp 415-420 , ESTEC, ESA

Hirsch, C. & Hakimi, N. (1995): Preconditioning Methods for Time Marching Navier-Stokes Solvers. Solution Techniques for Large Scale CFD Problems, CMAS, John Wiley & Sons, pp 333-353.

Hirsch, C. & Khodak, A.E. (1995): Application of Different Turbulent Models for Duct Flow Simulation with Reduced and Full Navier-Stokes Equations, ASME Paper 95-GT-145

Hishida, M.; Nagano, Y.; Tagawa, M. (1986): Transport Processes of Heat and Momentum in the Wall Region of Turbulent Pipe Flow. Proc. Int. Heat Transfer Conf., San Francisco, Vol.3, pp 925-930, Hemisphere

Kays, W.M. & Crawford, M.E. (1980): Convective Heat and Mass Transfer. 2nd edition, Mc Graw Hill

Korotky, G.J. & Taslim, M.E. (1996): Rib Heat Transfer Coefficient Measurements in a Rib-Roughened Square Passage. ASME Paper 96-GT-356

Launder, B.E. & Spalding, D.B. (1974): The Numerical Computation of Turbulent Flows. Comp. Meth. Appl. Mech. Eng., Vol. 3, pp 269-289
Rau, G.; Çakan, M.; Moeller, D.; Arts, T. (1998): The Effect of Periodic Ribs on the Local Aerodynamic and Heat Transfer Performance of a Straight Cooling Channel. J. of Turbomachinery, ASME, Vol. 120, pp 368-375
Taslim, M.E. & Wadsworth, C.M. (1997): An experimental Investigation of the Rib Surface-Averaged Heat Transfer Coefficient in a Rib Roughened Square Passage. J. of Turbomachinery, ASME, Vol. 119, pp 381-388.
Yang, Z. & Shih, T.H. Shih (1993): New Time Scale Based k-ε Model for Near Wall Turbulence. AIAA J., Vol. 31, No 7

Paper Number: 39

Name of Discusser: H.B. Weyer, DLR Cologne

Question:
Would you be able – with your sophisticated facility end impressive measuring techniques – to study natural transition-dependent of free stream turbulence and its effects on heat transfer?

Answer:
This would depend on the type of flowfield. At low or moderate speed with reasonable boundary layer thickness, I would suggest LDA or any optical method with sufficient frequency response. At high speed, or in the case of thin boundary layers, I would use heat transfer measurements to get quantitative results. Hot films, in most cases, provide only “semi-quantitative” information, which is maybe not sufficient, e.g. for validation purposes.

Name of Discusser: P. Kotsiopoulos, Hellenic Air Force Academy Attiki, Greece

Question:
You mentioned the uncertainties associated to the measurements for the mean fluctuating values of temperature and velocity.
How do you evaluate these uncertainties?

Answer:
The uncertainties were evaluated according to the well established Klilne and Mc Clintok technique.